

Increased hypothalamic-pituitary-adrenal axis activity and hepatic insulin resistance in low-birth-weight rats.

Esben Buhl, Susanne Neschen, Shin Yonemitsu, Joerg Rossbacher, Dongyan Zhang, Katsutaro Morino, Allan Flyvbjerg, Pascale Perret, Varman Samuel, Jung Kim, et al.

► **To cite this version:**

Esben Buhl, Susanne Neschen, Shin Yonemitsu, Joerg Rossbacher, Dongyan Zhang, et al.. Increased hypothalamic-pituitary-adrenal axis activity and hepatic insulin resistance in low-birth-weight rats.. *AJP - Endocrinology and Metabolism*, American Physiological Society, 2007, 293 (5), pp.E1451-8. <10.1152/ajpendo.00356.2007>. <inserm-00379890>

HAL Id: inserm-00379890

<http://www.hal.inserm.fr/inserm-00379890>

Submitted on 10 Sep 2009

HAL is a multi-disciplinary open access archive for the deposit and dissemination of scientific research documents, whether they are published or not. The documents may come from teaching and research institutions in France or abroad, or from public or private research centers.

L'archive ouverte pluridisciplinaire **HAL**, est destinée au dépôt et à la diffusion de documents scientifiques de niveau recherche, publiés ou non, émanant des établissements d'enseignement et de recherche français ou étrangers, des laboratoires publics ou privés.

Increased Hypothalamic-Pituitary-Adrenal Axis Activity and Hepatic Insulin Resistance in Low Birth Weight Rats

Esben S. Buhl^{1,2,3}, Susanne Neschen³, Shin Yonemitsu³, Joerg Rossbacher³, Dongyan Zhang³, Katsutaro Morino³, Allan Flyvbjerg², Pascale Perret³, Varman Samuel³, Jung Kim⁴, Gary W. Cline³, and Kitt Falk Petersen^{1,3}*

¹ Department of Pharmacology, Faculty of Health Sciences, Medical Department M, University of Aarhus; ² Medical Research Laboratory, Aarhus University Hospital, Aarhus Sygehus, Aarhus, Denmark; and Departments of ³ Internal Medicine and ⁴ Pathology, Yale University School of Medicine, New Haven, Connecticut

* Address for correspondence: K. F. Petersen, Yale University School of Medicine, Dept. of Internal Medicine, Section of Endocrinology, Cedar St. 333, P. O. Box 208020, New Haven, CT 06520-8020 (e-mail: kitt.petersen@yale.edu).

Key Words: Low Birth Weight, Hepatic Insulin Resistance, Hypothalamic-Pituitary-Adrenal Axis

ABSTRACT

Individuals born with a low birth weight (LBW) have an increased prevalence of type 2 diabetes, but the mechanisms responsible for this association are unknown. Given the important role of insulin resistance in the pathogenesis of type 2 diabetes, we examined insulin sensitivity in a rat model of LBW due to intrauterine fetal stress. During the last 7 days of gestation, rat dams were treated with dexamethasone and insulin sensitivity was assessed in the LBW offspring by a hyperinsulinemic euglycemic clamp. The LBW group had liver-specific insulin resistance associated with increased levels of PEPCK expression. These changes were associated with pituitary hyperplasia of the ACTH secreting cells, increased morning plasma ACTH concentrations, elevated corticosterone secretion during restraint stress, and an ~70% increase in 24-h urine corticosterone excretion. These data support the hypothesis that prenatal stress can result in chronic hyperactivity of the hypothalamic-pituitary-adrenal axis, resulting in increased plasma corticosterone concentrations, upregulation of hepatic gluconeogenesis, and hepatic insulin resistance.

Key Words: gluconeogenesis; adrenocorticotrophic hormone; corticosterone; type 2 diabetes

INTRODUCTION

According to the barker hypothesis, harmful events taking place during the fetal period can induce life-long changes in different organs predisposing to development of disease (1). In accordance with this hypothesis, individuals born with a birth weight of less than 5.5 lbs [low birth weight (LBW)] are insulin resistant (3, 12, 15, 17, 22, 28, 30, 35) and have increased prevalence of type 2 diabetes (10, 15, 28). Additionally, these patients are also prone to exhibit impaired growth in childhood and early adulthood, which may be related to alterations in the growth hormone/IGF-I homeostasis (16, 18, 20). The mechanisms responsible for these changes associated with LBW are unknown. Recently, fetal stress and high plasma levels of glucocorticoids have been suggested (5, 27) to lead to hypothalamic pituitary-adrenal (HPA) axis hyperactivity, which after birth may result in chronically excessive adrenal glucocorticoid secretion, and an increased risk for the development of type 2 diabetes. However, these findings have been contrasted by other studies that have found no change (32) or decreased HPA axis activity (21) in LBW rat models. To examine the mechanism and potential role of the HPA axis in causing LBW-associated insulin resistance, we assessed insulin-stimulated liver and muscle glucose metabolism, total IGF-I, and IGF-binding proteins (IGFBPs), as well as HPA axis activity in a rat model of stress-induced LBW.

MATERIALS AND METHODS

Animals. From *day 7* of gestation, pregnant female Sprague-Dawley rats (Charles River, Wilmington, MA) were housed singly under temperature (22–23°C)- and light-controlled (12:12-h light-dark cycle) conditions. On *day 14* of gestation, rats were randomized into three groups: control, dexamethasone treatment, or foster mother group. From *day 14* to *day 21* of gestation, a daily subcutaneously injection of dexamethasone (Sigma Aldrich) was given as 150 µg/kg dissolved in 4% ethanol/saline solution at a concentration of 200 µg/ml as previously described (25). Control dams were injected with a similar volume of the 4% ethanol/saline solution. Foster mothers were left undisturbed until delivery. To avoid postnatal influence of either

dexamethasone or saline treatment, newborn pups were transferred to a healthy, noninjected foster mother immediately after birth. Six to eight pups/dam were fostered. Rats were weaned at 3 wk of age, and further studies were performed in male rats only. The studies were approved by the Yale University Institutional Animal Care and Use Committee.

The animals were divided into groups to undergo the different parts of these studies: In the first group, $n = 10$ LBW and $n = 12$ control rats underwent the hyperinsulinemic euglycemic clamp studies. The second group of $n = 10$ LBW and $n = 12$ control rats underwent assessment of 24-h urinary corticosterone excretion, followed 3 days later by blood collection for measurements of fasting plasma concentrations of IGF-I, IGFBPs, triglycerides, cholesterol, HDL cholesterol, and basal liver and epididymal fat pad tissue collection. The third group of $n = 10$ LBW and $n = 12$ control rats underwent the restraint stress test experiment, followed 3 days later by measurements of 8 AM plasma ACTH levels. In the fourth group of $n = 9$ LBW and $n = 10$ control rats, the pituitary immunohistochemical staining and quantification of ACTH-positive cells were performed.

Twenty-four-hour urine collection. To minimize stress, rats were housed singly in metabolic cages for 1 h on 2 successive days prior to the 24-h urine collection. Urine was collected in plastic tubes and immediately centrifuged at 4,000 rpm for 10 min at 4°C to remove contaminants from debris of food and feces. Afterwards, total urine volume was determined and urine kept frozen at -20°C until further analysis.

Restraint stress test. Rats were placed in a restrainer for 90 min, and tail vein blood samples were collected at 0, 15, 30, 45, 60, 75, and 90 min, immediately centrifuged at 8,000 rpm for 20 s, and stored at -20°C until further analysis. Plasma corticosterone concentrations were assessed using a commercially available kit (MP Biomedicals, East Lansing, MI).

Urine corticosterone concentrations. Corticosterone levels in urine were determined by liquid chromatography-tandem mass spectrometry using an internal standard (cat. no. D3009; Medical Isotopes, Pelham, NH). Total 24-h urine corticosterone excretion was subsequently calculated by multiplying urine-corticosterone concentration and total 24-h urine volume.

Plasma ACTH levels. At 8 AM, after an overnight fast, resting rats were quickly anesthetized with isoflurane, and blood was collected by cardiac puncture and immediately transferred to a precooled Eppendorf tube (4°C) pretreated with aprotine and phenylmethylsulphonyl fluoride to neutralize protease activity. The samples were subsequently centrifuged for 30 s at 4°C, quick-

frozen on dry ice, and stored at -70°C until further analysis. Plasma ACTH concentrations were measured by a commercially available kit (MP Biomedicals).

In vivo glucose metabolism. Five to 7 days before the studies, indwelling catheters were placed into the jugular vein extending into the right atrium for blood collections and into the left carotid artery extending into the aortic arch for infusions as previously described (29). Catheters were tunneled subcutaneously and externalized at the neck region of the rat, filled with a polyvinylpyrrolidone heparine solution, and closed with tape. Rats were fasted overnight for 12 h prior to the clamp experiment and were awake, unstressed, and moving freely during the study. The 2-h basal period was begun with a primed (10 μCi), continuous (0.10 $\mu\text{Ci}/\text{min}$) infusion of D-[3- ^3H]glucose, and baseline venous blood was collected during the final 30 min for determination of plasma concentrations of glucose and insulin and for D-[3- ^3H]glucose-specific activity. The 135-min euglycemic hyperinsulinemic clamp was initiated with a primed (200 mU/kg body wt), continuous insulin infusion at a rate of $4 \text{ mU}\cdot\text{kg}^{-1}\cdot\text{min}^{-1}$ (Humulin R-100; Eli Lilly, Indianapolis, IN) and an additional primed (30 μCi), continuous (0.30 $\mu\text{Ci}/\text{min}$) infusion of D-[3- ^3H]glucose to maintain steady plasma D-[3- ^3H]glucose-specific activity. Plasma glucose levels were kept at 100 mg/dl by a variable infusion of 20% D-glucose. Blood samples were collected every 5 min during the final 45 min of the clamp for determination of plasma steady-state concentrations of glucose, insulin, and D-[3- ^3H]glucose-specific activity. At the end of the clamp rats were euthanized by an intravenous injection of pentobarbital sodium, and liver, epididymal fat, and gastrocnemius muscles were quickly freeze-clamped in situ with aluminum tongs precooled in liquid nitrogen and stored at -80°C .

Plasma metabolite and hormone concentrations. Plasma glucose concentrations were measured on a Glucose Analyzer II (Beckman Instruments, Fullerton, CA). Plasma insulin concentrations were measured using a RIA kit (Linco Research). Plasma samples for the determination of steady-state-specific activity of D-[3- ^3H]glucose were deproteinized by 0.3 N barium hydroxide, followed by 0.3 N zinc sulfate. Samples were centrifuged for 5 min at 12,000 rpm, and the supernatant was dried overnight. Dry samples were resuspended in filtered water, and D-[3- ^3H]glucose activity was counted in a liquid scintillation analyzer (Packard 2200CA; Canberra Packard, Pangbourne, UK). Fasting plasma levels of total cholesterol, high-density lipoprotein (HDL) cholesterol, and triglycerides were measured on a general plasma analyzer (Cobas Mira; Roche).

Serum IGF-I. Serum IGF-I concentrations were measured after extraction with acid-ethanol (30 μ l of serum and 750 μ l of acid-ethanol), by RIA using a polyclonal rabbit antibody (Nichols Institute Diagnostics, San Capistrano, CA), and with recombinant human IGF-I as standard (Amersham International, Bucks, UK) as previously described (9). Monoiodinated IGF-I [125 I-(Tyr31)-IGF-I] was obtained from Novo Nordisk (Bagsværd, Denmark). Intra- and interassay coefficients of variation were between 5 and 10% for both assays.

Western ligand blotting for determination of serum IGFBPs. SDS-PAGE and Western ligand blotting (WLB) were performed as previously described (7, 13). Two microliters of serum was subjected to SDS-PAGE (10% polyacrylamide) under nonreducing conditions. On WLB (with 125 I-IGF-I as the ligand), IGFBP-3 appears as a 38- to 42-kDa doublet band corresponding to the intact acid-stable IGF binding subunit of IGFBP-3, IGFBP-2 appears as a 34-kDa band, IGFBP-1 appears as a 30-kDa band, and IGFBP-4 appears as a 24-kDa band. Western ligand blots were quantified by densitometry with a Shimadzu CS-9001 PC dual wavelength flying spot scanner, and the relative densities were expressed as pixel density.

Glucose transport activity in muscle. To estimate insulin-stimulated muscle and fat glucose transport activity, an intravenous priming dose of 20 μ Ci 2-[1- 14 C]deoxyglucose was administered at $t = 90$ min during the euglycemic hyperinsulinemic clamp. Plasma-specific activity of 2-[1- 14 C]deoxyglucose was measured at 91, 93, 95, 100, 105, 115, 125, and 135 min and with the concentrations of plasma glucose used to calculate glucose uptake activity in gastrocnemius muscle and epididymal fat. The tissues were diluted 10-fold in water, homogenized, and placed in a heat block at 100°C for 10 min. After being cooled to room temperature, samples were centrifuged for 5 min, and the supernatant was diluted 1:15 with water. The total activity of 2-[1- 14 C]deoxyglucose was calculated as the sum of phosphorylated (intracellular) and unphosphorylated (extracellular) fractions of 2-[1- 14 C]deoxyglucose. These fractions of 2-[1- 14 C]deoxyglucose were separated on anion exchange chromatography columns (cat. no. 731-6211; Bio-Rad Laboratories, Hercules, CA) for determination of intracellular 2-[1- 14 C]deoxyglucose. Tissue-specific glucose transport activities were calculated from the amount of intracellular 2-[1- 14 C]deoxyglucose, plasma 2-[1- 14 C]deoxyglucose activity, and mean plasma glucose concentrations.

Quantitative RT-PCR for hepatic mRNA expression of phosphoenolpyruvate carboxykinase, IGF-I, IGFBP-1, and the glucocorticoid receptor. mRNA was isolated by use of mRNeasy kit

(Qiagen, Valencia, CA) for liver and adipose tissue, respectively, in combination with DNAase digestion. Two micrograms of RNA was reverse transcribed with an oligo prime (Stratagene, La Jolla, CA), and a PCR reaction was performed with a DNA Engine OptiControl 2 System (MJ Research, Boston, MA) by use of SYBR Green quantitative PCR dye kit. The primers for the different genes were phospho*enol*pyruvate carboxykinase (PEPCK): 5' CAG GAA GTG AGG AAG TTT GTG G 3' (forward) and 5' ATG ACA CCC TCC TCC TGC AT 3' (reverse); IGF-I: 5' TGG GCT TTG TTT TCA CTT CG 3' (forward) and 5' GGT CTC TGG TCC GGC TGT 3' (reverse); IGFBP-1: 5' GTG GAA TGC CAT TAG CAC CT 3' (forward) and 5' ATG TCT CGC ACT GTT TGC TG 3' (reverse); and glucocorticoid receptor: 5' TGT ATC CCA CAG ACC AAA GCA 3' (forward) and 5' AAT CCT CAT TCG TGT TCC CTT C 3' (reverse). Product specificity was confirmed by running products on an agarose gel, and mRNA levels (ΔC_T values) were expressed relative to 18S, using the comparative method (24).

Immunohistochemical staining for ACTH in pituitaries. All brain fixations took place between 9 and 11 AM. after isoflurane anesthesia. The right ventricle of the heart was opened to ensure venous outflow, and the abdominal aorta and vena cava were clamped to prevent perfusion of the lower carcass. The brain tissue was prefixed for 15 min by an arterial infusion of 2% paraformaldehyde in cold 0.1 M Na acetate (pH = 6.5). After the prefixation, the brain was fixed in situ by a 25-min infusion of cold 2% paraformaldehyde in 0.1% glutaraldehyde in 0.1 M Na borate (pH = 8.5). The skull was opened and the pituitary isolated and fixed overnight in a superfixation solution. For the ACTH immunohistochemical examination the paraffin was removed from the 6-micron-thick paraffin sections, which were treated with 3% H₂O₂ for 3 min, washed with Tris-buffered saline, and covered with 2% normal goat serum for 30 min. Sections were incubated overnight at 4°C with primary antibody [mouse anti-ACTH antibody (1:300, Dako-M3501)] and, on the following morning, rinsed with Tris-buffered saline and incubated with biotinylated anti-mouse antibody for 1 h, followed by a Tris-buffered saline rinse and 1-h incubation with a streptavidin-peroxidase complex. Immunoreactivity of the tissue was evaluated after treatment with diaminobenzidine, a chromogen, and hematoxylin counterstaining. Four representative regions for each pituitary were examined in a blinded fashion, a digital picture was taken of each of these four regions of each pituitary, and the ACTH-positive cells were counted using a counting grid. The number of ACTH-positive cells is the average of the four pictures and expressed in percent of the average number of ACTH-positive cells in control pituitaries.

Glucose metabolism. Basal and insulin-stimulated rates of glucose production were calculated as the ratio of D-[3-³H]glucose specific activity of infusate to the plasma-specific D-[3-³H]glucose activity, and rates of hepatic glucose production and insulin-stimulated peripheral glucose uptake were calculated as previously described (29).

Statistical analyses. Comparisons between LBW and control rats were performed using the two-tailed Student's *t*-test. *P* values of <0.05 were considered statistically significant. Data are given as means ± SE.

RESULTS

Body weight and fasting plasma metabolites. At birth, the LBW group weighed 13% less than the control group [control: 6.6 ± 0.1 g (*n* = 100) vs. LBW: 5.8 ± 0.1 g (*n* = 68), *P* < 0.00001]. However, the LBW group gradually caught up, and at the time of study, at 40 days of age, the weights of the LBW and control groups were similar [control: 151.1 ± 10.3 g (*n* = 10) vs. LBW: 167.9 ± 5.3 g (*n* = 12), *P* < 0.20]. Fasting plasma concentrations of glucose [control: 105.6 ± 3.0 mg/dl (*n* = 10) vs. LBW: 112.4 ± 2.5 mg/dl (*n* = 12), *P* < 0.10] and insulin [control: 6.2 ± 0.8 mU/l (*n* = 15) vs. LBW: 10.1 ± 1.9 mU/l (*n* = 16), *P* < 0.05] tended to be higher in the LBW compared with the control group, although this difference was not statistically significant. Fasting plasma concentrations of total cholesterol [control: 74.0 ± 3.3 mg/dl (*n* = 10) vs. LBW: 76.9 ± 3.8 mg/dl (*n* = 8), *P* < 0.57], HDL cholesterol [control: 42.2 ± 1.7 mg/dl (*n* = 10) vs. LBW: 42.7 ± 2.1 mg/dl (*n* = 8), *P* < 0.85], and triglycerides [control: 60.5 ± 8.0 mg/dl (*n* = 10) vs. LBW: 56.6 ± 8.8 mg/dl (*n* = 8), *P* < 0.75] were similar between the groups. The ratio of the epididymal fat pad to body weight was similar between the control and LBW rats [controls: 4.65 ± 0.56 g fat/kg body wt (*n* = 10) vs. 5.56 ± 0.46 g fat/kg body wt (*n* = 10), *P* < 0.22].

In vivo glucose metabolism. Rates of fasting hepatic glucose production [HGP; control: 8.1 ± 0.8 mg·kg⁻¹·min⁻¹ (*n* = 10) vs. LBW: 9.3 ± 0.6 mg·kg⁻¹·min⁻¹ (*n* = 12), *P* < 0.23] and the basal expression of PEPCK mRNA [control (*n* = 10): 100.0 ± 8.7% of control levels (*n* = 10) vs. LBW: 114.0 ± 12.7% (*n* = 10), *P* < 0.37] were similar between the groups.

During the hyperinsulinemic euglycemic clamp, plasma glucose concentrations (Fig. 1A), D-[3-³H]glucose-specific activity (Fig. 1B), and insulin concentrations were similar in the two groups

[controls: 101.4 ± 10.2 mU/l ($n = 7$) vs. LBW: 109.2 ± 15.6 mU/l ($n = 6$), $P < 0.68$], but the rate of glucose infusion required to maintain euglycemia during the clamp was 34% lower ($P < 0.01$) in the LBW group compared with the controls, reflecting insulin resistance in the LBW group (Fig. 1C). Since the rates of insulin-stimulated peripheral glucose uptake were similar in the two groups (Fig. 1D), and accordingly, rates of insulin-stimulated 2-deoxyglucose uptake in the gastrocnemius muscle also were similar among the groups (data not shown), this insulin resistance in the LBW rats could be attributed entirely to the liver. There was an almost complete lack of suppression of HGP during the clamp in the LBW, in contrast to the almost complete suppression of HGP in the control group (Fig. 2, A and B). Rates of glucose uptake in the epididymal fat rates of were similar between the groups (data not shown).

The hepatic insulin resistance was accompanied by a lack of suppression of PEPCK mRNA expression during the clamp (Fig. 2C). Thus, after insulin stimulation, PEPCK expression was 2.8-fold higher in the LBW than in the control rats ($P < 0.05$).

Fasting circulating levels of IGF-I and IGFbps. Basal plasma concentrations of total IGF-I were similar in the LBW and the control groups. However, concentrations of IGFBP-1 were $17.6 \pm 2.5\%$ higher in the LBW group compared with controls ($P < 0.03$). Plasma concentrations of IGFBP-2, -3, or -4 were similar between the groups (data not shown).

Basal hepatic gene expression. The elevated plasma concentration of IGFBP-1 in the LBW group was associated with an approximately twofold elevation of the hepatic IGFBP-1 mRNA expression. In accordance with the plasma concentrations of total IGF-I, the hepatic IGF-I mRNA expression was similar between the LBW and control groups. In addition, mRNA expressions of glucocorticoid receptor were also the same in the LBW and control groups, respectively (data not shown).

Twenty-four-hour urinary corticosterone excretion. The 24-h urine corticosterone excretion in the LBW group was 73% higher in the LBW than the control group ($P < 0.05$; Fig. 3A).

Restraint stress test. Fasting plasma corticosterone concentrations were similar in the controls [136 ± 32 ng/ml ($n = 6$)] and LBW [74 ± 24 ng/ml ($n = 6$), $P < 0.16$] groups. The stress-induced increment above basal plasma corticosterone concentrations was increased by ~118 and ~120% in the LBW group at 75 and 90 min, respectively (Fig. 3B). In accordance with this, the total area under the curve from 60 to 90 min was ~106% higher in the LBW than in the control group ($P < 0.05$; Fig. 3B, right).

Immunohistochemical staining for ACTH. On histological examination, the pituitary gland appeared normal [Fig. 4, A (controls) and B (LBW)], but there were ~20% more ACTH positive cells in the pituitaries of the LBW rats (Fig. 4B), as counted in four randomly chosen sections from the lateral pituitary lobes of each animal ($P < 0.05$; Fig. 4C).

Plasma ACTH concentrations. Fasting plasma ACTH concentrations at 8 AM were increased approximately twofold in the LBW rats compared with the control rats ($P < 0.05$; Fig. 4D).

DISCUSSION

This model of LBW is the result of chronic fetal glucocorticoid exposure by daily dexamethasone administration to the dam throughout the last 7 days of pregnancy. This fetal glucocorticoid exposure causes reduced fetal growth and LBW, and it is associated with the development of glucose intolerance and hypertension (25, 26) comparable with the common observations in LBW humans (6, 14, 22, 30, 31). To study the earliest established metabolic effects of LBW, male rats were studied at 40 days of age (e.g., juvenile rats), when plasma concentrations of glucose were normal but plasma insulin levels tended to be increased, reflecting whole body insulin resistance.

These studies demonstrate that LBW, in a rat model of fetal glucocorticoid exposure, results in hepatic insulin resistance accompanied by impaired insulin suppression of mRNA expression of PEPCK, suggesting impaired insulin suppression of hepatic gluconeogenesis. Furthermore, these alterations were associated with increased activity of the HPA axis, as reflected by increased plasma ACTH levels, an ~70% increase in 24-h urinary corticosterone excretion, and a prolonged increase in plasma corticosterone levels during restraint stress. Consistent with these findings, pituitary sections showed hyperplasia of the ACTH-secreting cells.

In an earlier study, Nyirenda et al. (25) found that fetal exposure to dexamethasone resulted in LBW, fasting hyperglycemia, and glucose intolerance after an oral glucose challenge. In addition, they found that hepatic expression of mRNA PEPCK and PEPCK activity were increased. However, neither hepatic insulin sensitivity nor HPA axis activity were assessed in that study.

In our model of LBW, rats had normal fasting plasma glucose concentrations and normal rates of hepatic glucose production but severe hepatic insulin resistance, as reflected by impaired

suppression of hepatic glucose production during the hyperinsulinemic euglycemic clamp compared with the control rats. This hepatic insulin resistance may be attributed to upregulation of hepatic gluconeogenesis, as reflected by increased hepatic expression of PEPCK mRNA, although additional contributions from increased hepatic glycogenolysis cannot be ruled out. Hepatic insulin resistance has been found in another model of LBW (32) due to intrauterine stress caused by ligation of the maternal uterine arteries. In this model, hepatic insulin resistance was associated with decreased hepatic insulin-stimulated insulin receptor substrate-2 and Akt2 phosphorylation and increased expression of PEPCK and glucose-6-phosphatase mRNA. However, in contrast to our LBW model, these pups had normal birth weight and increased rates of basal hepatic glucose production. In addition, those authors (32) did not find alterations in plasma corticosterone concentrations and speculated that hepatic insulin resistance in this model of LBW could possibly be ascribed to increased oxidative stress due to overproduction of reactive oxygen species in the liver. In vivo assessment of the HPA axis is very difficult in awake rodents, and it is likely that the inability of these workers to detect increases in plasma corticosterone concentrations in their LBW model may be due to the oscillatory nature of corticosterone secretion and possible stress associated with blood collection, which may obscure differences between groups. To avoid these possible confounding effects we assessed 24-h urinary glucocorticoid excretion in our study, since this measurement provides an integrated picture of adrenal glucocorticoid production, and it can be done in an awake animal with a minimal amount of stress. Using this approach, we found that 24-h urinary corticosterone excretion was increased by ~70% in the LBW group compared with the control group. These changes were associated with pituitary hyperplasia of the ACTH-secreting cells, increased morning plasma ACTH concentrations, and elevated corticosterone secretion during restraint stress. Taken together, these data suggest that the increased corticosterone production in the LBW rats in our study can be attributed to increased HPA axis activity.

It is well established that increased adrenal glucocorticoid production can result in increased rates of hepatic gluconeogenesis due to increased expression of PEPCK (2, 11), and in this study we show that hepatic insulin resistance was associated with increased mRNA expression of PEPCK. Inhibition of gluconeogenesis is much less responsive to insulin than inhibition of net hepatic glycogenolysis, and increased gluconeogenic flux in this LBW model can likely explain the observed hepatic insulin resistance during the hyperinsulinemic euglycemic clamp (4).

The juvenile LBW rats studied in this paper further displayed increased plasma concentrations of IGFBP-1 but normal concentrations of IGF-I and IGFBP-2, -3, and -4. These findings on plasma were further supported by an elevated hepatic IGFBP-1 mRNA expression together with normal hepatic IGF-I mRNA expression. Together, these data suggest a reduction in the ratio of total IGF-I relative to the total plasma protein binding capacity for IGF-I and, hence, a possibly decreased content of the free bioactive IGF-I. Similar disturbances compatible with diminished free IGF-I concentrations have been seen in humans born with LBW (8, 19) and in animal models of LBW (23, 33, 34); together, these changes may play a role for the postnatal impairment in length growth known to be associated with fetal growth retardation. The regulation of IGF-I and IGFBPs is known to be influenced by glucocorticoid stimulation, and the elevation of IGFBP-1 mRNA expression and plasma concentration may reflect increased hepatic corticosterone stimulation.

Hepatic mRNA expressions of glucocorticoid receptor were the same in LBW and control rats. Also, the expression of 11 β -hydroxysteroid dehydrogenase-1, an enzyme known to be a crucial rate limiting step of hepatic glucocorticoid metabolism, has previously been shown to be normal (25). Together, these findings suggest that circulating glucocorticoids are capable of stimulating the liver in a completely normal manner, and therefore, it is also feasible that the considerably elevated corticosterone levels exhibited by this LBW model play an important role in the changes seen regarding hepatic insulin action and hepatic gene expressions, respectively.

Taken together, these data support the hypothesis that increased HPA axis activity and hepatic insulin resistance, potentially due to increased hepatic gluconeogenesis, are major factors responsible for the impaired insulin action associated with LBW due to prenatal glucocorticoid exposure. Given these results, it will be important to determine whether insulin resistance, due to increased activity of the HPA axis, occurs in LBW humans due to prenatal stress.

ACKNOWLEDGMENTS

We thank Dr. Jan Frystyk, Karen Mathiassen, and Kirsten Nyborg, Aarhus Sygehus; Aida Groszmann and Andrea Belous; and Yale University General Clinical Research Center Core Laboratory for expert assistance. We also thank Dr. Sten Lund (Aarhus Sygehus) for stimulating discussions.

GRANTS

These studies were supported by grants from the US Public Health Service (R01-AG-23686, R01-DK-40936, P01-DK-068229, and P30-DK-45735). E. S. Buhl was supported by a fellowship award to Dr. Ole Schmitz, Department of Pharmacology, Faculty of Health Sciences, University of Aarhus and Aarhus Sygehus, and by National Institute on Aging Grant R01-AG-23686.

REFERENCES

1. Barker DJ, Record RG. The relationship of the presence of disease to birth order and maternal age. *Am J Hum Genet* 19: 433–449, 1967.
2. Barthel A, Schmoll D. Novel concepts in insulin regulation of hepatic gluconeogenesis. *Am J Physiol Endocrinol Metab* 285: E685–E692, 2003.
3. Carlsson S, Persson PG, Alvarsson M, Efendic S, Norman A, Svanstrom L, Ostenson CG, Grill V. Low birth weight, family history of diabetes, and glucose intolerance in Swedish middle-aged men. *Diabetes Care* 22: 1043–1047, 1999.
4. Chiasson JL, Liljenquist JE, Finger FE, Lacy WW. Differential sensitivity of glycogenolysis and gluconeogenesis to insulin infusions in dogs. *Diabetes* 25: 283–291, 1976.
5. Clark PM. Programming of the hypothalamo-pituitary-adrenal axis and the fetal origins of adult disease hypothesis. *Eur J Pediatr* 157, Suppl 1: S7–S10, 1998.
6. Dabelea D, Pettitt DJ, Hanson RL, Imperatore G, Bennett PH, Knowler WC. Birth weight, type 2 diabetes, and insulin resistance in Pima Indian children and young adults. *Diabetes Care* 22: 944–950, 1999.
7. Flyvbjerg A, Kessler U, Dorka B, Funk B, Orskov H, Kiess W. Transient increase in renal insulin-like growth factor binding proteins during initial kidney hypertrophy in experimental diabetes in rats. *Diabetologia* 35: 589–593, 1992.
8. Greenwood PL, Bell AW. Consequences of intra-uterine growth retardation for postnatal growth, metabolism and pathophysiology. *Reprod Suppl* 61: 195–206, 2003.
9. Gronbaek H, Volmers P, Bjorn SF, Osterby R, Orskov H, Flyvbjerg A. Effect of GH/IGF-I deficiency on long-term renal changes and urinary albumin excretion in diabetic dwarf rats. *Am J Physiol Endocrinol Metab* 272: E918–E924, 1997.
10. Hales CN. Fetal and infant growth and impaired glucose tolerance in adulthood: the “thrifty phenotype” hypothesis revisited. *Acta Paediatr Suppl* 422: 73–77, 1997.
11. Hanson RW, Reshef L. Regulation of phosphoenolpyruvate carboxykinase (GTP) gene expression. *Annu Rev Biochem* 66: 581–611, 1997.
12. Hofman PL, Regan F, Jackson WE, Jefferies C, Knight DB, Robinson EM, Cutfield WS. Premature birth and later insulin resistance. *N Engl J Med* 351: 2179–2186, 2004.

13. Hossenlopp P, Seurin D, Segovia-Quinson B, Hardouin S, Binoux M. Analysis of serum insulin-like growth factor binding proteins using western blotting: use of the method for titration of the binding proteins and competitive binding studies. *Anal Biochem* 154: 138–143, 1986.
14. Jaquet D, Gaboriau A, Czernichow P, Levy-Marchal C. Insulin resistance early in adulthood in subjects born with intrauterine growth retardation. *J Clin Endocrinol Metab* 85: 1401–1406, 2000.
15. Jaquet D, Leger J, Levy-Marchal C, Czernichow P. Low birth weight: effect on insulin sensitivity and lipid metabolism. *Horm Res* 59: 1–6, 2003.
16. Jensen RB, Chellakooty M, Vielwerth S, Vaag A, Larsen T, Greisen G, Skakkebaek NE, Scheike T, Juul A. Intrauterine growth retardation and consequences for endocrine and cardiovascular diseases in adult life: does insulin-like growth factor-I play a role? *Horm Res* 60, *Suppl 3*: 136–148, 2003.
17. Jornayvaz FR, Selz R, Tappy L, Theintz GE. Metabolism of oral glucose in children born small for gestational age: evidence for an impaired whole body glucose oxidation. *Metabolism* 53: 847–851, 2004.
18. Kajantie E. Insulin-like growth factor (IGF)-I, IGF binding protein (IGFBP)-3, phosphoisoforms of IGFBP-1 and postnatal growth in very low-birth-weight infants. *Horm Res* 60, *Suppl 3*: 124–130, 2003.
19. Kajantie E, Dunkel L, Rutanen EM, Seppala M, Koistinen R, Sarnesto A, Andersson S. IGF-I, IGF binding protein (IGFBP)-3, phosphoisoforms of IGFBP-1, and postnatal growth in very low birth weight infants. *J Clin Endocrinol Metab* 87: 2171–2179, 2002.
20. Kanaka-Gantenbein C, Mastorakos G, Chrousos GP. Endocrine-related causes and consequences of intrauterine growth retardation. *Ann NY Acad Sci* 997: 150–157, 2003.
21. Lesage J, Blondeau B, Grino M, Breant B, Dupouy JP. Maternal undernutrition during late gestation induces fetal overexposure to glucocorticoids and intrauterine growth retardation, and disturbs the hypothalamo-pituitary adrenal axis in the newborn rat. *Endocrinology* 142: 1692–1702, 2001.
22. Levitt NS, Lambert EV, Woods D, Hales CN, Andrew R, Seckl JR. Impaired glucose tolerance and elevated blood pressure in low birth weight, nonobese, young South African adults: early programming of cortisol axis. *J Clin Endocrinol Metab* 85: 4611–4618, 2000.

23. Manikkam M, Crespi EJ, Doop DD, Herkimer C, Lee JS, Yu S, Brown MB, Foster DL, Padmanabhan V. Fetal programming: prenatal testosterone excess leads to fetal growth retardation and postnatal catch-up growth in sheep. *Endocrinology* 145: 790–798, 2004.
24. Neschen S, Morino K, Hammond LE, Zhang D, Liu ZX, Romanelli AJ, Cline GW, Pongratz RL, Zhang XM, Choi CS, Coleman RA, Shulman GI. Prevention of hepatic steatosis and hepatic insulin resistance in mitochondrial acyl-CoA:glycerol-sn-3-phosphate acyltransferase 1 knockout mice. *Cell Metab* 2: 55–65, 2005.
25. Nyirenda MJ, Lindsay RS, Kenyon CJ, Burchell A, Seckl JR. Glucocorticoid exposure in late gestation permanently programs rat hepatic phosphoenolpyruvate carboxykinase and glucocorticoid receptor expression and causes glucose intolerance in adult offspring. *J Clin Invest* 101: 2174–2181, 1998.
26. O'Regan D, Kenyon CJ, Seckl JR, Holmes MC. Glucocorticoid exposure in late gestation in the rat permanently programs gender-specific differences in adult cardiovascular and metabolic physiology. *Am J Physiol Endocrinol Metab* 287: E863–E870, 2004.
27. O'Regan D, Welberg LL, Holmes MC, Seckl JR. Glucocorticoid programming of pituitary-adrenal function: mechanisms and physiological consequences. *Semin Neonatol* 6: 319–329, 2001.
28. Ong KK, Dunger DB. Perinatal growth failure: the road to obesity, insulin resistance and cardiovascular disease in adults. *Best Pract Res Clin Endocrinol Metab* 16: 191–207, 2002.
29. Samuel VT, Liu ZX, Qu X, Elder BD, Bilz S, Befroy D, Romanelli AJ, Shulman GI. Mechanism of hepatic insulin resistance in non-alcoholic fatty liver disease. *J Biol Chem* 279: 32345–32353, 2004.
30. Stefan N, Weyer C, Levy-Marchal C, Stumvoll M, Knowler WC, Tataranni PA, Bogardus C, Pratley RE. Endogenous glucose production, insulin sensitivity, and insulin secretion in normal glucose-tolerant Pima Indians with low birth weight. *Metabolism* 53: 904–911, 2004.
31. Veening MA, van Weissenbruch MM, Delemarre-Van De Waal HA. Glucose tolerance, insulin sensitivity, and insulin secretion in children born small for gestational age. *J Clin Endocrinol Metab* 87: 4657–4661, 2002.
32. Vuguin P, Raab E, Liu B, Barzilai N, Simmons R. Hepatic insulin resistance precedes the development of diabetes in a model of intrauterine growth retardation. *Diabetes* 53: 2617–2622, 2004.

33. Woodall SM, Bassett NS, Gluckman PD, Breier BH. Consequences of maternal undernutrition for fetal and postnatal hepatic insulin-like growth factor-I, growth hormone receptor and growth hormone binding protein gene regulation in the rat. *J Mol Endocrinol* 20: 313–326, 1998.
34. Woodall SM, Breier BH, Johnston BM, Gluckman PD. A model of intrauterine growth retardation caused by chronic maternal undernutrition in the rat: effects on the somatotrophic axis and postnatal growth. *J Endocrinol* 150: 231–242, 1996.
35. Yajnik CS. Early life origins of insulin resistance and type 2 diabetes in India and other Asian countries. *J Nutr* 134: 205–210, 2004.

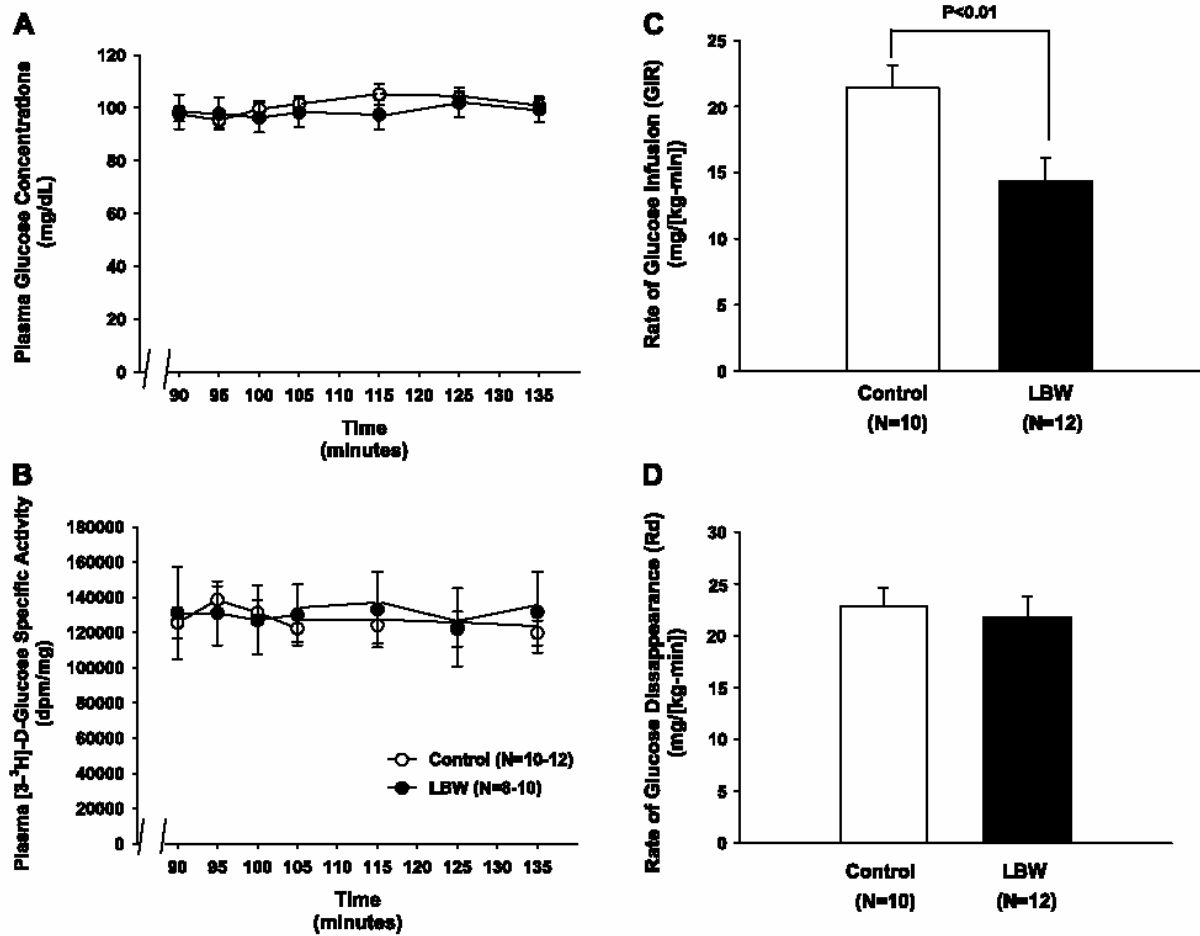


Fig. 1. Insulin-stimulated glucose metabolism in 40-day-old control and low-birth-weight (LBW) rats. *A*: plasma glucose concentrations during the euglycemic hyperinsulinemic clamp. ○Controls; ●LBW. *B*: plasma [3-³H]glucose-specific activity during the euglycemic hyperinsulinemic clamp. ○Controls; ●LBW. *C*: rates of insulin-stimulated glucose infusion (GIR; *n* = 10–12). *D*: rates of glucose disappearance (Rd; *n* = 10–12).

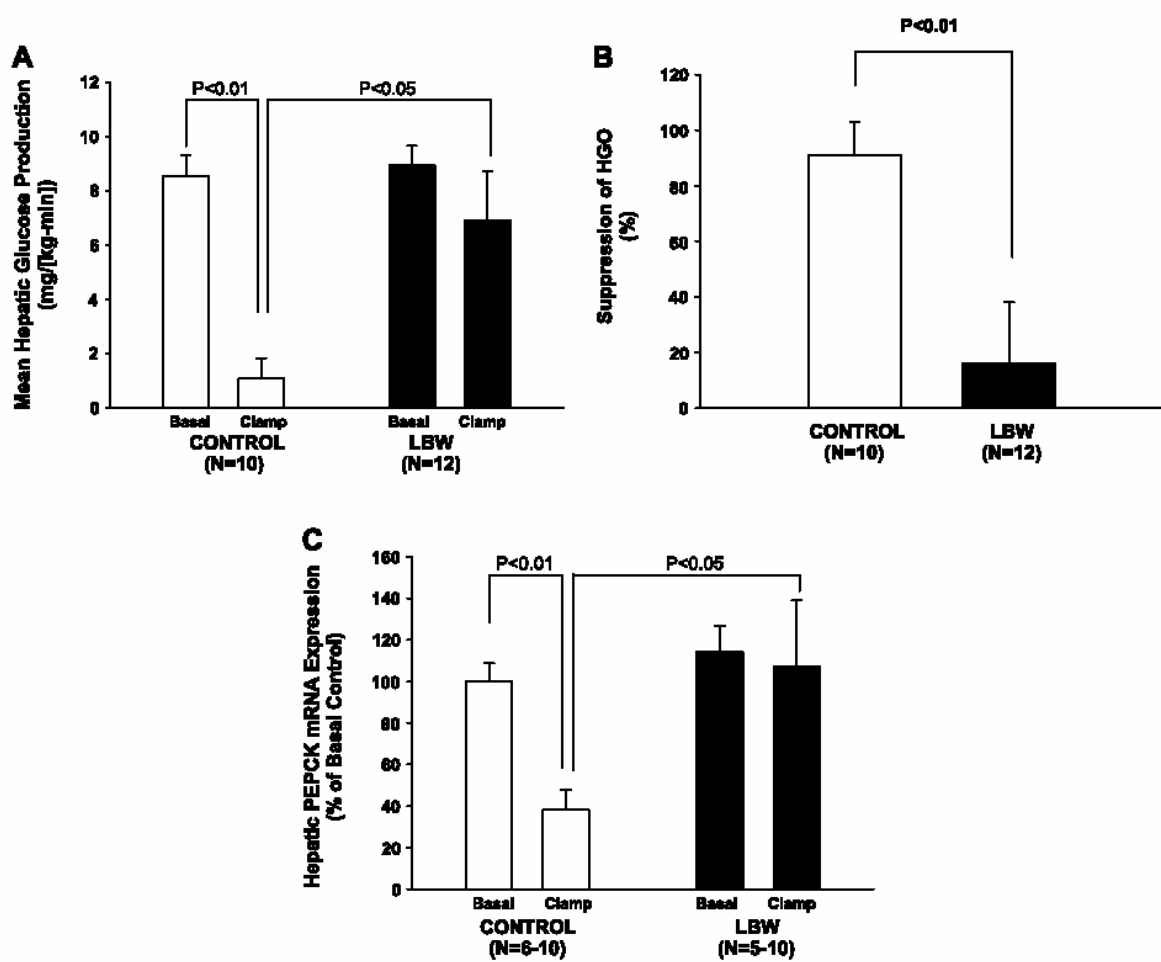


Fig. 2. Hepatic glucose metabolism. *A*: rates of fasting and insulin-stimulated hepatic glucose production (HGP) in control and LBW rats ($n = 10-12$). *B*: %Insulin suppression of HGO ($n = 10-12$). *C*: fasting and insulin-stimulated hepatic phosphoenolpyruvate carboxykinase (PEPCK) mRNA expression in control and LBW rats ($n = 5-10$).

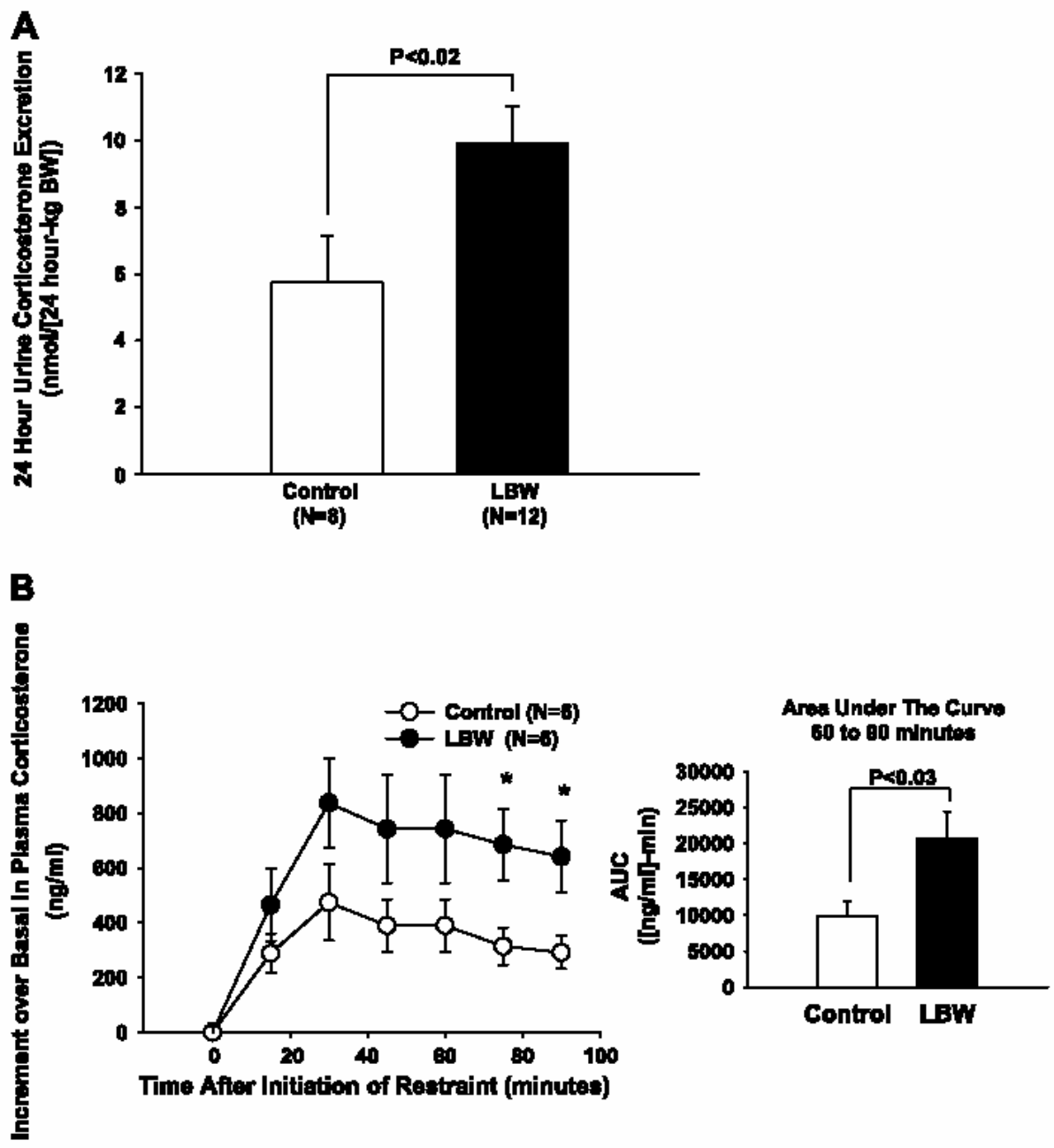


Fig. 3. Corticosterone secretion in control and LBW rats. *A*: 24-h urinary corticosterone excretion in control and LBW rats ($n = 8-12$). *B*: plasma corticosterone increase above basal during restraint stress tests ($n = 6$). * $P < 0.04$, control vs. LBW.

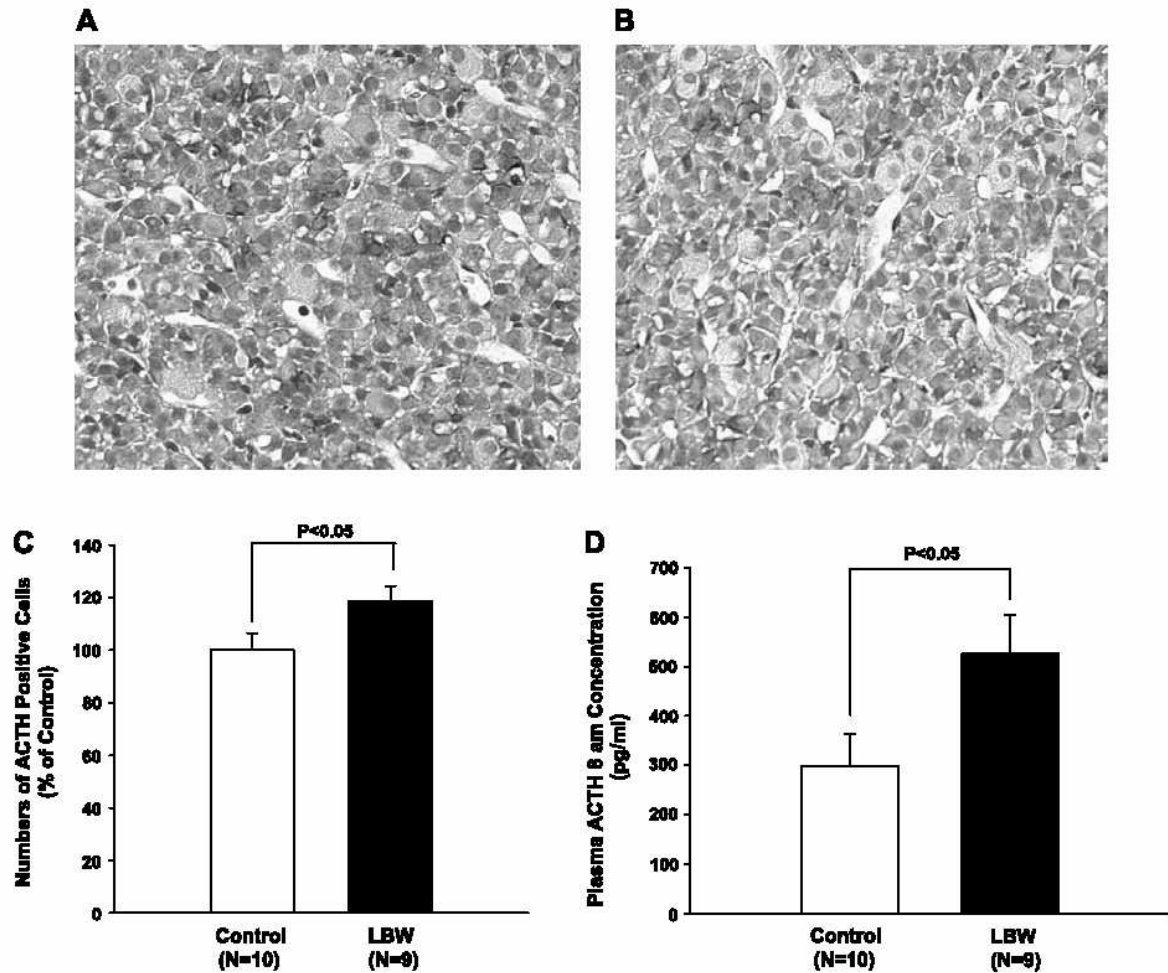


Fig. 4. Morphology and number of pituitary ACTH-secreting cells and fasting at 8 AM. Plasma ACTH concentrations in control and LBW rats. *A*: immunohistochemical staining for ACTH in the lateral lobe of the pituitary in a control rat (magnification: 1:100, 57 ACTH-positive cells in shown section). *B*: immunohistochemical staining for ACTH in the pituitary lateral lobe of a LBW rat (magnification: 1:100, 64 ACTH-positive cells in shown section). *C*: quantification of ACTH-positive cells in a random area of the lateral lobe of the pituitary in LBW rats. Number of ACTH positive cells expressed as %number of ACTH positive cells in control lateral pituitary lobe ($n = 9-10$). *D*: plasma ACTH concentrations at 8 AM, after 14 h of fasting, in control and LBW rats ($n = 9-10$).